# Detection of slope failure in the 2016 Kumamoto Earthquake using optical satellite imagery

13T0268W Costanza Althea Nyigor
Supervisors : Fumio Yamazaki, Wen Liu

## 1. Introduction

A $M_J$ 6.5 earthquake hit Kumamoto region of Kyushu Island, Japan on 14th April 2016 at 21:26 pm local time. Subsequently, a larger earthquake with a magnitude of 7.3 occurred on 16th April 2016 at 1:25 am local time. The depth of the epicenter of the mainshock is 10 km. This earthquake triggered many landslides in the mountainous areas of the Kumamoto region, mainly in the Mount Aso area. Bridges and roads were damaged in Mashiki Town, Minami Aso Village and Nishihara Village, resulting in major disruption of the traffic network. In the case of natural disasters occurring in mountainous regions, it is very difficult to collect information from the ground. In order to prevent damages due to disasters from getting worse, it is necessary to assess details of disasters quickly. In this case, remote sensing technology using images obtained from satellites and aircrafts is effective to grasp damages[1) 2)].

In this study, the optical satellite images of Landsat-8 and ASTER taken before earthquake and after earthquake are used to extract slope failures in the Kumamoto region. The slope failures are detected by the two methods, and their results are verified by comparing to the visual interpretation.

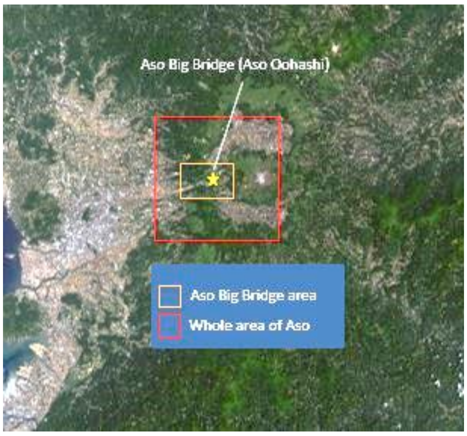


**Figure 1** Study area in Kumamoto region, Japan

## 2. Study area and data used

Figure 1 shows the focus study area, mainly near the Aso Great Bridge area. Most slope failures occurred around these mountainous areas.

The Landsat-8 and ASTER satellite images taken before and after the earthquake are obtained to extract the slope failures. The pre-event Landsat-8 image is taken on 5th May 2015 while the post-event image is taken on 23rd May 2016. From ASTER sensor, the pre-event image is taken on 7th May 2013 while for the post-event is taken on 20th April 2016.

## 3. Methodology

Firstly, the slope failures are extracted from the Landsat-8 images. The pre- and post-event images are pre-processed by doing registration, radiometric calibration and pan-sharpening approaches. The original resolution of the Landsat-8 image is 30 m and a 15 m resolution multi-bands image can be obtained after the pan-sharpening. In a slope failure, the surface with dense vegetation changes to bare land due to the movement of soil and vegetation from high to low ground. Because of this, the Normalized Difference Vegetation Index (NDVI) is utilized to obtain slope failures. The NDVI values are first calculated from the pre- and post-event images. Then the differences between the two NDVIs are obtained. The area with the NDVI values decrease could be indicated as a slope failure. Digital elevation model (DEM) is also applied to improve the extracted results. The areas with the slope less than 10 degrees are removed from the results.

Supervised classifications are also carried out for the pre- and post-event images to extract slope failures. The areas that is classified as the bare land in the post-event image but classified as the other land-covers in the pre-event image might be slope failures.

The same approaches are applied to the images taken by ASTER. Finally, the extracted results are compared to the truth data published by PASCO, and the accuracy assessment is carried out.

## 4. Detection of slope failure using Landsat-8 images

The extraction of slope failures in the Aso Oohashi area is carried out using NDVI. This area has a lot of slopes, causing a big landslide near the Aso Big Bridge and damaging roads and the bridge. Using the NDVI decrease, most of the slope failure could be extracted in the whole study area. However, several small slope failures are difficult to be detected due to the low resolution of the satellite images. Then, the supervised classification was applied to the pre- and post-event images. The largest slope failure is extracted successfully by comparing the landcover change. However, some areas are wrongly extracted because of the low-resolution and also seasonal change. The results of slope failures extraction using the NDVI values and the supervised classifications method are shown in Figure 2.

In the whole study area (red frame in Figure 1), 3.13 km$^2$ is obtained as the slope failures using NDVI method. In the Aso Great Bridge area (yellow frame in Figure 1), a total slope failure area of 0.67 km$^2$ is obtained from NDVI whereas 1.74 km$^2$ is detected by the supervised classification. Accuracy evaluation is then conducted and the result is shown in Table 1.

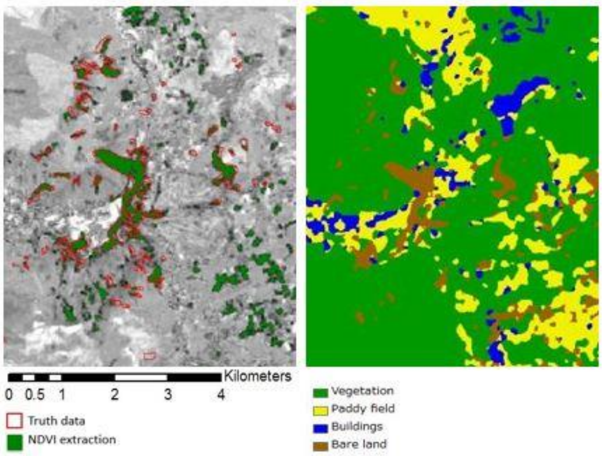


**Figure 2** Detected slope failures from the Landsat-8 images using NDVI (left) and the supervised classification (right)

**Table 1** Accuracy evaluation for the results from the Landsat-8 images

| Accuracy | NDVI difference extraction | Supervised classification |
|---|---|---|
| Producer accuracy | 37.5% | 55.3% |
| User accuracy | 65.8% | 37.6% |

## 5. Detection of slope failure using ASTER images

The slope failures around the Aso Great Bridge are first extracted by the NDVI values and supervised classification. The results are shown in Figure 3.

The result using NDVI values shows that most slope failures occur in the mountainous regions. Small-scale slope failures are also difficult to be detected due to 15m resolution. The extraction using the supervised classification is also carried out. Its result shows that a few areas which are not slope failures are classified as the bare lands in the post-event image. It is caused by the clear-up for crops, which is classified as bare land.

In the whole study area, 10.9 km$^2$ s obtained as the slope failures using NDVI method. In the Aso Great Bridge area, 1.33 km$^2$ is obtained as slope failures whereas 3.65 km$^2$ is detected by the supervised classification. Accuracy evaluation is conducted and the result is shown in Table 2.

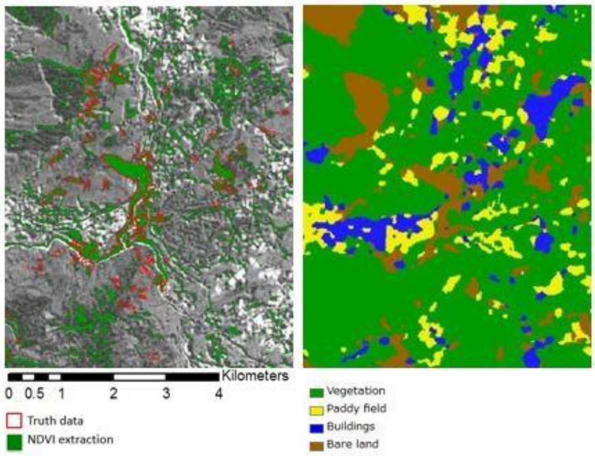


**Figure 3** Detected slope failures from the ASTER images using NDVI (left) and the supervised classification (right)

**Table 2** Accuracy evaluation for the results from the ASTER images

| Accuracy | NDVI difference extraction | Supervised classification |
|---|---|---|
| Producer accuracy | 29.0% | 40.3% |
| User accuracy | 38.5% | 17.3% |

## 6. Conclusion

In this study, the detection of the slope failures using Landsat-8 and ASTER images were conducted. The extraction using the Landsat-8 images shows a better result than the one using the ASTER images. Although the ASTER images have higher resolution, the pre- and post-event images were taken in different seasons. The different seasons gives a huge impact on the extraction using the NDVI difference. Thus, the pre- and post-event images taken under the same season would give a better result for the extraction of slope failure.

## References

1) Ishide Takahiro, Yamazaki Fumio: Detection of slope failures using ALOS/AVNIR-2 Images for the 2008 Iwate-Miyagi Inland Earthquake, Japan Association for Earthquake Engineering Journal, 10th Publication, No.3, 2010
2) Risako Tsuchida, Wen Liu, Yamazaki Fumio: Detection of landslides in the 2015 Gorkha, Nepal earthquake using satellite imagery, Japan Remote Sensing Conference, Publication No.60, 2016.